Mathematical Support of the Vessel Information and Risk Control Systems

Serhii Zinchenko[1[0000-0001-5012-5029]], captain Oleh Tovstokoryi[2[0000-0003-3048-0028]], Pavlo Nosov[3[0000-0002-5067-9766]], Ihor Popovych[4[0000-0002-1663-111X]], Vitaliy Kobets[5[0000-0002-4386-4103]], Gennadii Abramov[6[0000-0003-0333-8819]]

[1,2,3,6] Kherson State Maritime Academy, Ushakova avenue 20, Kherson, 73000, Ukraine
[4,5] Kherson State University, Universytetska st. 27, Kherson,73003, Ukraine

[1]srz56@ukr.net, [2]otovstokory@gmail.com, [3]pason@ukr.net, [4]ihorpopovych999@gmail.com, [5]vkobets@kse.org.ua, [6]gennadabra@gmail.com

Abstract. The article discusses the issues of mathematical support of the Information and Risk Control System for the offshore vessel operating in high risk areas near oil or gas platforms, other large moving objects. Vessels operating in high-risk areas are equipped with dynamic positioning systems and excessive control, which allows to increase the reliability, maneuverability and quality of control. Minimally excessive control structure with two stern Azimuth Control Devices (ACD) is considered. This structure is the last "frontier" to provide three-dimensional vessel control, therefore it is interesting in practical use. The control surfaces for this structure were built, their extreme values and level lines were analyzed. To dispensation redundancy, three control splitting algorithms were considered, analytical expressions for control splitting were obtained. There was carried out a comparative analysis of the considered splitting algorithms between themselves and the prototype according to the minimum $Risk$ - criterion. A comparative analysis showed that the splitting algorithm used in the prototype are special cases of the considered algorithms for dispensation redundancy. There were found controls that provide a "clean" rotation of the vessel without lateral force, which are not present in prototype. There were built control algorithms that provide complex vessel movements according to the minimum $Risk$ - criterion in automatic mode. Operability and efficiency of the algorithmic and software of the vessel control system operating in high risk areas, verified by mathematical modeling at imitation modeling stand.

Keywords: Information and Risk Control System , high-risk areas, offshore vessel, excessive control, control splitting, Pivot Point

1 Introduction and related work

According to the United Kingdom Protection and Indemnity (UK P & I) Club, the human factor accounts for 89-96% of collisions with ships, 84-88% of tanker accidents, 79% of landings when towing vessels and costs the marine industry about $ 541 million USA per year [1].

Studying the causes of these accidents, experts concluded that the main cause of risks is related to the human factor (HF). The HF influence on the vessel control was considered in the works of many authors, for example [1–6] and others.

To minimize the HF risk, IMO has developed and is constantly improving the International Convention on Standards of Training and Certification and Watch keeping for Seafarers, 1978 (STCW). In article [5], the results of the Master Pilot training in Kherson State Maritime Academy conducted within the framework of this standard are presented.

Further attempts to reduce HF risk are associated with the implementation of the Decision Support System (DSS). DSS can also be considered as Risk-Informed Systems. In such systems, the skipper still makes the final decision on the control of the vessel, which means that HF remains in the control loop - a part with partially undefined behavior, that generates a certain percentage of errors and has large delays in processing and transmitting information [7-9].

The next stage is the development of automatic control systems that perform control tasks without human intervention. Human functions in such systems are reduced only to monitoring control processes. In automatic control systems, the HF link is absent, which gives them great advantages. This is especially true for offshore vessels like Platform Supply / Support Vessel (PSV), Offshore Supply / Support Vessel (OSV), Diving Support Vessel (DSV), Remote Operated Vessel (ROV) and others.
Such vessels are subject to increased requirements for reliability, maneuverability and quality of control [10-12]. To fulfill these requirements, offshore vessels are equipped with dynamic positioning systems (DP – system) , active control devices (azimuth control devices (ACD) [13-14], bow and stern thrusters), have redundancy in the measurement and control channels. Control redundancy is a very important characteristic of a vessel, as it improves not only reliability, but also maneuverability, control quality and also reduces the risks of occurrence and development of adverse situations. The issues of using excessive structures for control were previously considered by the authors in their works.

So, article [14] describes manually controlling the movement of a vessel with the excessive structure of two stern ACD, bow and stern thrusters, and also with only two stern ACD. A structure with two stern ACD can occur when thrusters fail through clogging with sand or silt. In addition, this structure is the last “frontier” to provide three-dimensional vessel control, therefore it is of particular interest. One of the authors of this article, captain Tovstokoryi, worked on a similar vessel (anchor tug AHT Jascon 11 for pipe layer Jascon 30) in the waters of Nigeria.

Fig. 1 shows the author's photos of the anchor tug AHT Jascon 11 (IMO 9386847) and its stern ACD.

a b

Fig. 1. Anchor tugboat AHT Jascon 11 and its stern ACD

Fig. 2 shows the author's photos of the pipe layer Jascon 30 (IMO 9420655).

a b

Fig. 2. Pipe layer Jascon 30

Article [15] explores the problems of the distribution of the thrust force of an autonomous underwater vehicle engine between redundancy number of propulsors using the presented control splitting scheme. At the same time, an excessive number of propulsors was also used to increase the reliability of the system as a whole due to parry failures. The results were confirmed by computer simulation.

In article [16], the author considers the control of the angular position of the spacecraft using the excess structure of power gyroscopes. The presence of redundancy allows not only to increase the reliability of the control system as a whole, but also to optimize the control and unloading processes of power gyroscopes.

In article [17] there were considered issues of controlling the unloading of the flywheels of a control system for the angular orientation of a spacecraft. For a minimally redundant system of flywheels and electromagnetic executive equipment of the unloading system that create an additional external moment, control algorithms were synthesized that guarantee asymptotic stability to the zero solution of model equations describing the movement of the flywheels. The operability of the proposed algorithms and the features of the unloading process were investigated by the example of the controlled angular motion of spacecraft while stabilizing the triaxial orbital orientation.

In article [18] there was considered the use of angular redundancy for planning and optimizing the path of welding torch movement in various complex media. Efficiency strategies have been introduced, such as a heuristic domain sampling strategy, a collision verification strategy. The proposed algorithm is effective in solving complex planning problems when the weld passes in tight places. The experiment confirmed that the algorithm proposed by the authors can not only find a path free from collisions with obstacles in various complex environments, but also optimize the angle of the welding torch according to the established criterion.

The manual [19] describes three modern dynamic positioning systems: Navis, Marine Technologies and Rolls Royce.These systems allow to automatically maintain a given course, hold the set position, perform linear movements between the indicated points, perform complex vessel movement (longitudinal, lateral and rotational at the same time) in manual mode and also warn the skipper about the risks involved.

Fig. 3. Lowering the basket with the turn at the Pivot Point

Risk reduction is achieved through the organization optimal control of the vessel, including using Pivot Point (PP) [20]. At PP is no lateral speed of the vessel, which is convenient for raising or lowering the basket with the turn to this point.

Fig. 3 shows the moment of lowering the basket with the turn at the PP. PP is also used for optimal maneuvering around high risk areas, as well as in many other cases [21-24].

2 Methodology

The object of research is the processes of vessel automatic control with a minimally excessive coplanar structure of two stern ACD, using the criterion of minimum risk.

The subject of research is the method and algorithms, using the criterion of minimum risk for vessel automatic control with a minimally excessive coplanar structure of two stern ACD.

The purpose of research is to develop a method and algorithms of Information and Risk Control System, allowing to use the risk criterion for automatic control of the vessel.

During the research there were used methods of analysis and synthesis, methods of automatic control theory, risk assessment and reduction methods, numerical integration methods, mathematical modeling methods, experiment methods.

Fig. 4 shows the minimally redundant coplanar structure of two stern ACD with the indicated ACD positions in the linked coordinate system (LCS).

The beginning of the LCS is located in the center O of the vessel rotation, the axis OX_1 of the LCS lies in the diametrical plane and is directed to the bow of the vessel, the axis OY_1 of the LCS is perpendicular to the diametrical plane and is directed to the starboard side, the axis OZ_1 of the LCS complements the system to the "right" one. Position ACD_1 in LCS is (-a, -b, 0), position ACD_2 in LCS is (-a, b, 0). Valid control area ACD_1 is $|P_1| < P_{max}$, $|\alpha_1| < \pi$, valid control area ACD_2 is $|P_2| < P_{max}$, $|\alpha_2| < \pi$.

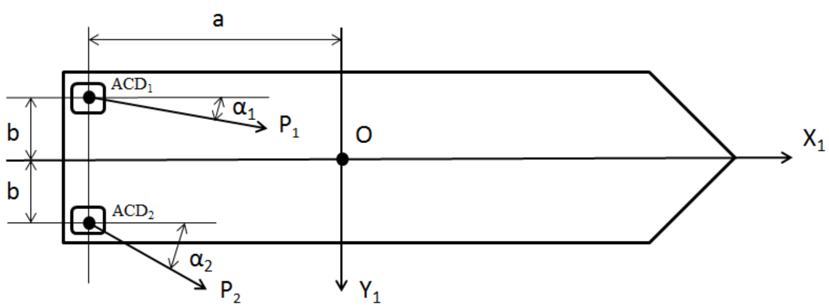

Fig. 4. The minimally excessive coplanar structure of two stern ACD

It is required to develop a method and algorithms for the vessel automatic control with minimally excessive coplanar structure of two stern ACD (Fig.4), allowing to reduce the risk of maneuvering around the platform.

The problem is solved in the on-board controller of the vessel's control system constantly, with the on-board controller clock cycle, in several stages: evaluation of the control vector to compensate for external forces and moment or for implementation of the required maneuver, selection of a control splitting scheme that is best for the obtained evaluation, formation of controls using the selected scheme.

For the control structure shown in Fig. 4, the equations of forces and moments in projections on LCS axis will have the form

$$P_x = P_1 \cos\alpha_1 + P_2 \cos\alpha_2, \quad (1)$$

$$P_y = P_1 \sin\alpha_1 + P_2 \sin\alpha_2, \quad (2)$$

$$M_z = P_1 b\cos\alpha_1 - P_2 b\cos\alpha_2 - P_1 a\sin\alpha_1 - P_2 a\sin\alpha_2, \quad (3)$$

where P_x, P_y, M_z are the required forces and moment in projections on the axis of the LCS. From equations (1) - (3) we can find the required control parameters $P_1, P_2, \alpha_1, \alpha_2$ corresponding to them. As can be seen from equations (1) - (3), the control structure has four independent control parameters $P_1, P_2, \alpha_1, \alpha_2$ and three constraint equations (1) - (3), which means that there is minimal control redundancy. Redundancy in control allows us to get the same values of the required forces and moments P_x, P_y, M_z for different sets of control parameters $P_1, P_2, \alpha_1, \alpha_2$ or controls $\mathbf{P}_1 = (P_1\cos\alpha_1, P_1\sin\alpha_1, 0), \mathbf{P}_2 = (P_2\cos\alpha_2, P_2\sin\alpha_2, 0)$.

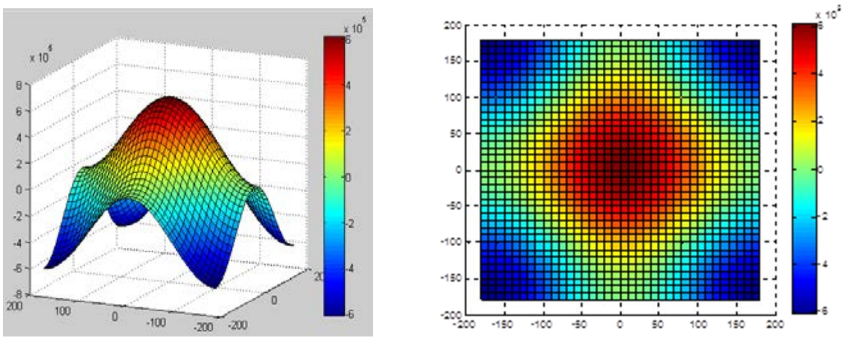

a b

Fig. 5. Surface $P_x = f_x(P_1^*, P_2^*, \alpha_1, \alpha_2)$

Fig. 5 shows the surface $P_x = f_x(P_1^*, P_2^*, \alpha_1, \alpha_2)$ defined by equation (1) as a function of angles α_1, α_2, for $P_1^* = P_{\max}, P_2^* = P_{\max}, |\alpha_1| < 180^\circ, |\alpha_2| < 180^\circ$. As can be seen from Fig. 5, in the region of admissible controls, the surface has one global maximum at the point $(\alpha_1 = 0, \alpha_2 = 0)$ and four global minimums at the points $(\alpha_1 = 180^\circ, \alpha_2 = 180^\circ)$, $(\alpha_1 = -180^\circ, \alpha_2 = 180^\circ)$, $(\alpha_1 = -180^\circ, \alpha_2 = -180^\circ)$, $(\alpha_1 = 180^\circ, \alpha_2 = -180^\circ)$, level lines are also visible, indicated by the same color on which $P_x = const$. So, on the level line shown in yellow $P_x = 1{,}5 \times 10^5$ (see color bar), and the level line $P_x = 0$ runs approximately along the border of light green and light blue.

Similarly, Fig. 6 shows the surface $P_y = f_y(P_1^*, P_2^*, \alpha_1, \alpha_2)$ for $P_1^* = P_{max}, P_2^* = P_{max}, |\alpha_1| < 180^\circ, |\alpha_2| < 180^\circ$.

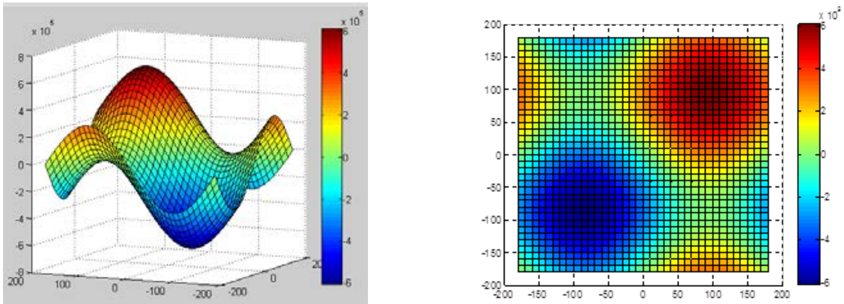

a b

Fig. 6. Surface $P_y = f_y(P_1^*, P_2^*, \alpha_1, \alpha_2)$

As can be seen from this figure, in the region of admissible controls, the surface has one global maximum at point $(\alpha_1 = 90^\circ, \alpha_2 = 90^\circ)$ and one global minimum at point $(\alpha_1 = -90^\circ, \alpha_2 = -90^\circ)$, level lines $P_y = const$ and $P_y = 0$ are also visible at approximately the border of light green and light blue colors.

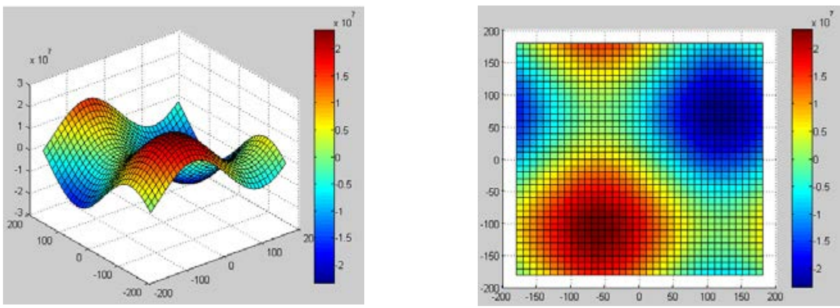

a b

Fig. 7. Surface $M_z = f_z(P_1^*, P_2^*, \alpha_1, \alpha_2)$

Fig. 7 shows the surface $M_z = f_z(P_1^*, P_2^*, \alpha_1, \alpha_2)$ for $P_1^* = P_{max}, P_2^* = P_{max}, |\alpha_1| < 180^\circ, |\alpha_2| < 180^\circ$.

As follows from equations (1) - (3) and the presented figures, the same values (level lines) can be implemented by different controls, which means that among these controls we can find the optimal control. To obtain optimal controls, it is required to split the total forces P_x, P_y and moment M_z into separate ACD controls $\mathbf{P}_1 = (P_1 \cos\alpha_1, P_1 \sin\alpha_1), \mathbf{P}_2 = (P_2 \cos\alpha_2, P_2 \sin\alpha_2)$, for which the adopted function of control quality assumes extreme value.

Unfortunately, it is not possible to solve such optimization problem in analytical form for system (1) - (3). Such solution can be obtained only in the on-board controller of the control system using numerical methods, for example [25-27]. However, the use of numerical methods for control splitting in real time is not safe, since their insufficiently correct tuning may exceed the permissible search time or not produce a result at all. Therefore, in practice, quasi-optimal splitting algorithms that allow an analytical solution are more preferable.

2.1 Control splitting algorithms

For some special cases that do not claim to be optimal, such analytical solutions can be obtained. For this, it is necessary to add an additional constraint equation in order to remove control redundancy in system (1) - (3**).**

Splitting algorithm 1. The constraint equation is $\alpha_1 = -\alpha_2$. Taking into account the constraint equation $\alpha_1 = -\alpha_2$, system (1) - (3) can be written as

$$P_x = (P_1 + P_2)\cos\alpha_1, \tag{4}$$

$$P_y = (P_1 - P_2)\sin\alpha_1, \tag{5}$$

$$M_z = (P_1 - P_2)b\cos\alpha_1 - (P_1 - P_2)a\sin\alpha_1. \tag{6}$$

From the system of equations (4) - (6) we obtain solutions (7) – (10)

$$\alpha_1 = arctg\,(\frac{P_y b}{M_z + P_y a}), \tag{7}$$

$$\alpha_2 = -\alpha_1. \tag{8}$$

$$P_1 = \frac{1}{2}(\frac{P_x}{\cos\alpha_1} + \frac{P_y}{\sin\alpha_1}), \tag{9}$$

$$P_2 = \frac{1}{2}(\frac{P_x}{\cos\alpha_1} - \frac{P_y}{\sin\alpha_1}). \tag{10}$$

Splitting algorithm 2. The constraint equation is $\alpha_1 = \alpha_2$. Taking into account the constraint equation $\alpha_1 = \alpha_2$, system (1) - (3) can be written as

$$P_x = (P_1 + P_2)\cos\alpha_1, \tag{11}$$

$$P_y = (P_1 + P_2) \sin \alpha_1 , \tag{12}$$

$$M_z = (P_1 - P_2) b \cos \alpha_1 - (P_1 + P_2) a \sin \alpha_1 . \tag{13}$$

From the system of equations (11) - (13) we obtain solutions (14) - (17)

$$\alpha_1 = arctg(\frac{P_y}{P_x}) , \tag{14}$$

$$\alpha_2 = \alpha_1 . \tag{15}$$

$$P_1 = \frac{P_x b + P_y a + M_z}{2b \cos \alpha_1} , \tag{16}$$

$$P_2 = \frac{P_x b - P_y a - M_z}{2b \cos \alpha_1} . \tag{17}$$

Splitting algorithm 3. The constraint equation is $\alpha_1 = 0$. Taking into account the constraint equation $\alpha_1 = 0$, system (1) - (3) can be written as

$$P_x = P_1 + P_2 \cos \alpha_2 , \tag{18}$$

$$P_y = P_2 \sin \alpha_2 , \tag{19}$$

$$M_z = P_1 b - P_2 b \cos \alpha_2 - P_2 a \sin \alpha_2 . \tag{20}$$

From the system of equations (18) - (20) we obtain solutions (21) – (24)

$$P_1 = \frac{P_x b + P_y a + M_z}{2b} . \tag{21}$$

$$\alpha_1 = 0 \tag{22}$$

$$\alpha_2 = arctg\,(\frac{P_y}{P_x - P_1}) . \tag{23}$$

$$P_2 = \frac{P_y}{\sin \alpha_2} . \tag{24}$$

2.2 Comparative analysis of splitting algorithms by *Risk* criterion.

The obtained analytical solutions of the control splitting algorithms were verified by mathematical modeling in EXEL. The result of mathematical modeling for the splitting algorithm $\alpha_1 = -\alpha_2$ is presented in Table 1. Control quality function $Risk = P_1^2 + P_2^2$ is equivalent to the power expended on control, and the control scheme, which provides less power to solve the task, is more efficient and has less risk when maneuvering around the platform.

Table 1. The results of mathematical modeling for the splitting algorithm $\alpha_1 = -\alpha_2$

(P_x, P_y, M_z)	α_1	α_2	P_1	P_2	$Risk$	Shema
(0,001;0,001;0,001)	7,816	-7,816	0,004	-0,003	0,000	
(1;0,001;0,001)	7,816	-7,816	0,508	0,501	0,509	
(0,001;1;0,001)	7,97	-7,97	3,607	-3,606	26,011	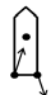
(0,001;0,001;1)	0,382	-0,382	0,076	-0,075	0,011	
(-1;0,001;0,001)	7,816	-7,816	-0,501	-0,508	0,509	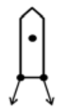
(0,001;-1;0,001)	7,97	-7,97	-3,606	3,607	26,009	
(0,001;0,001;-1)	-0,422	0,422	-0,067	0,068	0,009	

The result of mathematical modeling for the splitting algorithm $\alpha_1 = \alpha_2$ is presented in Table 2.

Table 2. The results of mathematical modeling for the splitting algorithm $\alpha_1 = \alpha_2$

(P_x, P_y, P_z)	α_1	α_2	P_1	P_2	*Risk*	Shema
(0,001;0,001;0,001)	45,0	45,0	0,006	-0,004	0,000	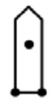
(1;0,001;0,001)	0,057	0,057	0,504	0,496	0,5	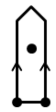
(0,001;1;0,001)	89,95	89,95	3572,0	-3571	$25,4e^{6}$	
(0,001;0,001;1)	45,0	45,0	0,107	-0,105	0,023	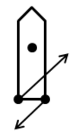
(-1;0,001;0,001)	-0,057	-0,057	-0,496	-0,504	0,5	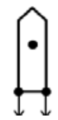
(0,001;-1;0,001)	-89,95	-89,95	-3571	3571	$25,4e^{6}$	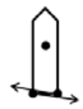
(0,001;0,001;-1)	45,0	45,0	-0,095	0,097	0,018	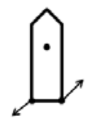

The results of mathematical modeling for the splitting algorithm $\alpha_1 = 0$ are presented in Table 3.

Table 3. The results of mathematical modeling for the splitting algorithm $\alpha_1 = 0$

(P_x, P_y, P_z)	α_1	α_2	P_1	P_2	*Risk*	Shema
(0,001;0,001;0,001)	0,0	-17,651	0,006	-0,004	0,000	
(1;0,001;0,001)	0,0	0,115	0,504	0,496	0,5	
(0,001;1;0,001)	0,0	-15,645	3,572	-3,708	26,511	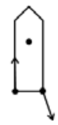
(0,001;0,001;1)	0,0	-0,769	0,076	-0,075	0,011	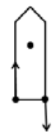
(-1;0,001;0,001)	0,0	-0,114	-0,496	-0,504	0,5	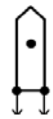
(0,001;-1;0,001)	0,0	-15,642	-3,571	3,709	26,509	
(0,001;0,001;-1)	0,0	0,838	-0,067	0,068	0,009	

Table 4 shows the *Risk* function values for the considered control splitting algorithms.

Table 4. Values of the $Risk$ function for the considered control splitting algorithms

(P_x, P_y, P_z)	$\alpha_1 = -\alpha_2$	$\alpha_1 = \alpha_2$	$\alpha_1 = 0$
(0,001;0,001;0,001)	0	0	0
(1;0,001;0,001)	0,509	0,5	0,5
(0,001;1;0,001)	26,011	25,4e^6	26,511
(0,001;0,001;1)	0,011	0,023	0,011
(-1;0,001;0,001)	0,509	0,5	0,5
(0,001;-1;0,001)	26,009	25,4e^6	26,509
(0,001;0,001;-1)	0,009	0,018	0,009

As can be seen from the data presented in Table 4, the splitting algorithm $\alpha_1 = \alpha_2$ is significantly inferior to the other two algorithms. So, the splitting algorithm $\alpha_1 = \alpha_2$ has a $Risk$ function value twice as high when generating "clean" torque around axis OZ_1 and is completely unsuitable for creating lateral forces along the axis OY_1. Splitting algorithms $\alpha_1 = -\alpha_2$ and $\alpha_1 = 0$ are approximately the same by the $Risk$ criterion, however, in the presence lateral force, the splitting algorithm $\alpha_1 = -\alpha_2$ is somewhat preferable, since it $Risk$ criterion 2% less than of splitting algorithm $\alpha_1 = 0$.

The results obtained are generalization of the available controls presented in the [14]. So, control 1 “Sailing slow ahead” on page 10 and control 3 “Sailing slow astern” on page 11 of the [14] coincide with the splitting algorithm $\alpha_1 = -\alpha_2$ for uniting the desired direction (1; 0; 0) and (-1; 0; 0). Control 2 “Sailing full ahead” on page 10 and control 4 “Sailing full astern on page 11 coincide with the splitting algorithm $\alpha_1 = \alpha_2$ or splitting algorithm $\alpha_1 = 0$ for uniting the desired direction (1; 0; 0) and (-1; 0; 0). Control 5 “Turning to port” and control 6 “Turning to starboard” on page 12 coincide with the splitting algorithm $\alpha_1 = 0$ for uniting the desired direction (1; 1; -1) and (1; -1; 1). Control 7 “Turning the stern to port” and control 8 “Turning the stern to starboard” on page 13 coincide with the splitting algorithm $\alpha_1 = \alpha_2$ for uniting the desired direction (-1; -1; 1) and (-1; 1; -1) . Control 9 “Normal stopping” on page 14 coincides with the splitting algorithm $\alpha_1 = -\alpha_2$, $\alpha_1 = \alpha_2$, $\alpha_1 = 0$ for uniting the desired direction (0; 0; 0). The control 10 “Emergency crash stop” on page 14 coincides with the splitting algorithm $\alpha_1 = -\alpha_2$ for the unit desired direction (-1; 0; 0). The controls 11 “Turning on the spot to port” and 12 “Turning on the spot to starboard” on page 15 coincide with the splitting algorithm $\alpha_1 = 0$ for uniting the desired direction (0; 1; -1) and (0; -1; 1). Additionally, there were found controls for the "pure" rotation (0; 0; 1) and (0; 0; -1) for all methods $\alpha_1 = -\alpha_2$, $\alpha_1 = \alpha_2$, $\alpha_1 = 0$. The controls "Walking the vessel slowly to port" on page 16 and the controls "Walking the vessel slowly to starboard" on page 18 are similar to the splitting algorithm $\alpha_1 = -\alpha_2$ for the unit vector of the desired direction (0; 1; 0) and (0; -1; 0). The control "Walking the vessel fast to port" on page 17 and the control "Walking the vessel fast to starboard" on page 19 are similar to the splitting algorithm $\alpha_1 = \alpha_2$ for uniting the desired direction (0; 1; 0) and (0; -1; 0).

3 Experiment, results and discussions

Operability and efficiency of the developed method and algorithms of the Information and Risk Control System was tested on Imitation Modeling Stand [28, 29], created by authors on the basis of the Navi Trainer 5000 simulator [30, 31], for several basic vessel movements: rotation around the Pivot Point, located in the center of rotation, stern of the vessel, in front of the vessel and behind the vessel, without longitudinal speed, as well as rotation around the Pivot Point, located in the rotation center, with longitudinal speed.

3.1 Imitation modeling stand

The imitation modeling stand is the Navi Trainer 5000 simulator itself as well as on-board controller simulator with mathematical support of the Information and Risk Control System. Between the on-board controller simulator and Navi Trainer 5000 simulator is organized information exchange in such way that the measured parameters of the vessel's state vector are read into the on-board controller simulator, processed in it according to the embedded algorithms for forming controls, the formed controls are transferred back to the Navi Trainer 5000 simulator for working out by the simulator vessel model. Thus, the Imitation Modeling Stand allows to work out the mathematical support of the Information and Risk Control System in a closed circuit with vessel simulator models.

For experiment in on-board controller simulator of Imitation Modeling Stand were flashed programs, based on the algorithm for evaluating the required control to implement a given motion or maintain a given position (PID controller)

$$P_x(n) = \frac{P_{\max}}{V_{\max}} V_x^*(n),$$

$$P_y(n) = k_y(y_m(n) - y^*(n)) + k_{V_y}(V_{ym}(n) - V_y^*(n)) + k_{\int y} \int (y_m(n) - y^*(n))dt,$$

$$M_z(n) = k_\psi(\psi_m(n) - \psi^*(n)) + k_\omega(\omega_{zm}(n) - \omega_z^*(n)) + k_{\int \psi} \int (\psi_m(n) - \psi^*(n))dt,$$

where $P_{\max,} V_{\max}, V_x^*$ are maximum thrust force, maximum vessel speed and specified longitudinal speed $V_{ym}(n), V_y^*(n)$ are measured and specified lateral speed of the vessel, $y_m(n), y^*(n)$ are measured and specified lateral movement of the vessel, $\omega_{zm}(n), \omega_z^*(n)$ are measured and specified yaw rate, $\psi_m(n), \psi^*(n)$ are measured and specified yaw angle, $k_y, k_{V_y}, k_{\int y}, k_\psi, k_\omega, k_{\int\psi}$ are PID controller gains, n is the number of information processing cycle in the on-board controller, algorithm for choosing the best splitting according to the *Risk* criterion for the required control estimate

Shema $(\alpha_1 = -\alpha_2)$, if Risk $(\alpha_1 = -\alpha_2)$ = min{Risk $(\alpha_1 = -\alpha_2)$,Risk $(\alpha_1 = 0)$, Risk $(\alpha_1 = \alpha_2)$ },

Shema $(\alpha_1 = 0)$, if Risk $(\alpha_1 = 0)$ = min{Risk $(\alpha_1 = -\alpha_2)$,Risk $(\alpha_1 = 0)$, Risk $(\alpha_1 = \alpha_2)$ },

Shema $(\alpha_1 = \alpha_2)$, if Risk $(\alpha_1 = \alpha_2)$ = min{Risk $(\alpha_1 = -\alpha_2)$,Risk $(\alpha_1 = 0)$, Risk $(\alpha_1 = \alpha_2)$ },

and algorithms (7-10), (14-17), (21-24) for splitting control and forming controls into actuators.

3.2 Testing the Information and Risk Control System on the example of automatic control of rotation around the Pivot Point without longitudinal speed.

This type of movement is used to "clean" rotation of the vessel around the bow, stern or any other point of the diametrical plane within the hull (for example, to lower or raise the basket with a turn) or outside the hull (for example, to maneuver around danger). Required movement can be implemented by setting the following programs

$$V_x^*(n) = 0,\ x^*(n) = R,\ V_y^*(n) = \omega_z^*(n)R,\ y^*(n) = V_y^*(n)n\Delta T,$$
$$\omega_z^*(n) = const,\ \psi^*(n) = \omega_z^*(n)n\Delta T,$$

where R is position of the Pivot Point relative to the vessel rotation center, ΔT is the information processing cycle in the on-board controller.

Fig. 8a shows automatic controlling the vessel rotation around the Pivot Point, located in the rotation center $(R = 0)$, in the absence of longitudinal speed.

Fig. 8b shows automatic controlling the vessel rotation around the Pivot Point, located in the stern $(R = -a)$, in the absence of longitudinal speed.

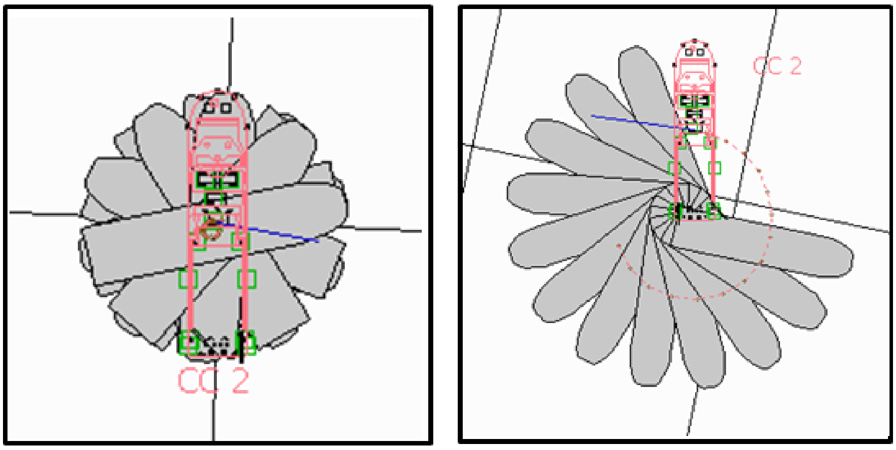

a b

Fig. 8. Automatic controlling of the vessel rotation around the Pivot Point, located in the rotation center $(R = 0)$ and in the stern ($(R = -a)$, in the absence of longitudinal speed.

Fig. 9a shows automatic controlling the vessel rotation around the Pivot Point, located in front of the bow.

Fig. 9b shows automatic controlling the vessel rotation around the Pivot Point, located behind the stern.

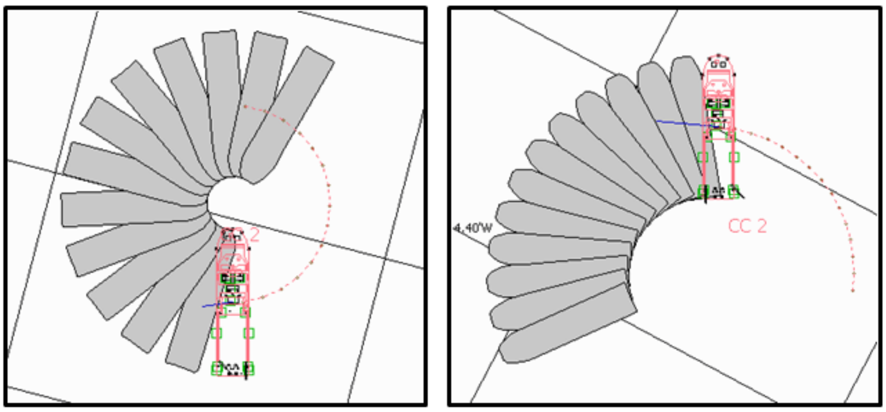

a b

Fig. 9. Automatic controlling of the vessel rotation around the Pivot Point, located in front of the bow and behind the stern

3.3 Testing the Information and Risk Control System on the example of automatic control of rotation around the Pivot Point with longitudinal speed.

This type of the movement is used to organize a curved trajectory, for example, when the vessel approaches the mooring object, course change with simultaneous development of lateral mismatch. Depending on the position of the Pivot Point, the movement can be organized with or without a drift angle. Required movement can be implemented by setting the following programs

$$V_x^*(n) = const,\ x^*(n) = V_x^*(n)n\Delta T, V_y^*(n) = \omega_z^*(n)R,\ y^*(n) = V_y^*(n)n\Delta T,$$
$$\omega_z^*(n) = const,\ \psi^*(n) = \omega_z^*(n)n\Delta T.$$

By setting the position of the Pivot Point, using the above equations, can obtain the program of vessel movement. For $\omega_z^*(n) = 0$ the vessel will move in a straight line with a zero drift angle. The zero drift angle can also be achieved if the Pivot Point is placed in the center of rotation ($R = 0$). In this case the vessel moves along a curved path without drift, which saves fuel by reducing hydrodynamic drag.

Fig. 10a shows the simulation results of the vessel movement without drift angle. The longitudinal speed of the vessel is 5,29 kn., the position of the Pivot Point coincides with the center of rotation.

Fig. 10b shows the simulation results of the vessel movement with drift angle. The longitudinal speed of the vessel is 0,91 kn., the Pivot Point is located between the center of rotation and the stern.

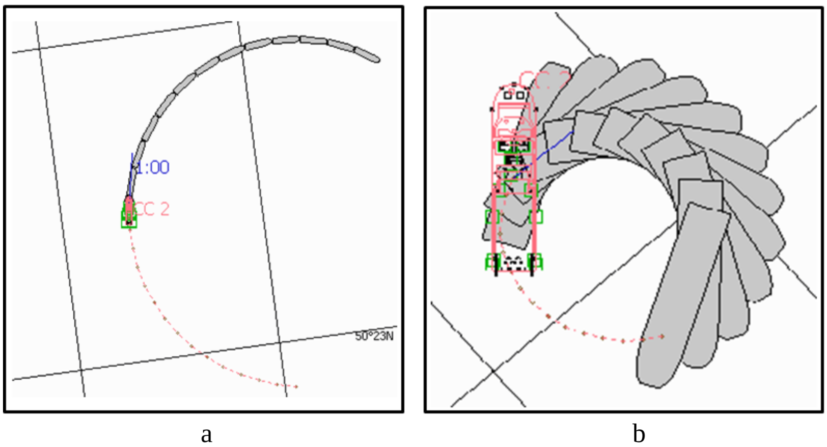

Fig. 10. Simulation results of the vessel movement around the Pivot Point with longitudinal speed

The simulation results confirm that considered mathematical support of the vessel Information and Risk Control System, in comparison with the known solutions, provides in automatic mode a quasi-optimal control of the complex movement of offshore vessel with a minimally excessive coplanar structure of two stern ASD. The ability to automatically control a vessel in high-risk areas allows to increase reliability, control accuracy, and also reduce the risk of adverse situations.

The proposed method and algorithms can be used in the development of mathematical support of the vessel Information and Risk Control Systems with minimally excessive coplanar ACD structure.

4 Conclusion

The article discusses the issues of mathematical support of the Information and Risk Control System for the offshore vessel, operating in high risk areas near oil or gas platforms. In the article were carried out the following studies:

- the analysis of literary sources devoted to issues of mathematical support of the Information and Risk Control System for the offshore vessel with excessive control were carried out, analogues and prototypes were found;
- as a result of the analysis, it was revealed that vessels operating in high risk areas are equipped with dynamic positioning systems and excessive control, which allows to increase the reliability, maneuverability and quality of control;
- the control surfaces $P_x = f_x(P_1^*, P_2^*, \alpha_1, \alpha_2)$, $P_y = f_y(P_1^*, P_2^*, \alpha_1, \alpha_2)$, $M_z = f_z(P_1^*, P_2^*, \alpha_1, \alpha_2)$ for minimally excess coplanar structure with two stern ACD were build, their extreme values and level lines were analyzed;
- to dispensation redundancy, three control splitting algorithms were considered, analytical expressions for control splitting were obtained;
- there was carried out a comparative analysis of the considered splitting algorithms between themselves and the prototype according to the minimum of *Risk* - criterion;
- a comparative analysis showed that the splitting algorithm used in the prototype are special cases of the considered algorithms for dispensation redundancy;
- there were found controls that provide a “clean” rotation of the vessel without lateral force, which are not present in prototype;
- there were developed method and algorithms for assessing the *Risk* degree for each considered splitting schemes are constructed depending on the required control, the choice of the best splitting scheme according to the minimum *Risk* degree, the formation of control using the selected scheme;
- there was written software for on-board controller simulator of Imitation Modeling Stand based on the developed method and algorithms;
- operability and efficiency of the method, algorithms and software were verified by mathematical modeling at Imitation Modeling Stand. The mathematical modeling confirmed the operability and efficiency of the developed method and algorithms and allows to recommend them for practical use.

References

1. Apostol – Mates, R., Barbu, A.: Human error – the main factor in marine accidents. Naval Academy Scientific Bulletin 19(2) (2016). DOI: 10.21279/1454-864X-16-I2-068
2. The Relation between Human Error and Marine Industry. https://www.marineinsight.com/marine-safety/the-relation-between-human-error-and-marine-industry/
3. Sotiralis, P., Ventikos, N. P., Hamann, R., Golyshev, P., Teixeira, A. P.: Incorporation of human factors into ship collision risk models focusing on human centered design aspects. Reliability Engineering & System Safety 156: 210-227 (2016). DOI: 10.1016/j.ress.2016.08.007
4. Luo, M., Shin, S.: Half-century research developments in maritime accidents: Future directions. Accident Analysis & Prevention 123: 448-460 (2019). DOI: 10.1016/j.aap.2016.04.010
5. Popovych, I. S., Cherniavskyi, V. V., Dudchenko, S. V., Zinchenko, S. M., Nosov, P. S., Yevdokimova, O. O., Burak, O. O., Mateichuk, V. M.: Experimental Research of Effective "The Ship's Captain and the Pilot" Interaction Formation by Means of Training Technologies. Revista ESPACIOS 41(11):30 (2020). http://www.revistaespacios.com/a20v41n11/20411130.html
6. Popovych, I., Blynova, O., Aleksieieva, M., Nosov, P., Zavatska, N., Smyrnova, O.: Research of Relationship between the Social Expectations and Professional Training of Lyceum Students studying in the Field of Shipbuilding. Revista ESPACIOS 40(33):21 (2019). https://www.revistaespacios.com/ a19v40n33/19403321.html
7. Nosov, P., Zinchenko, S., Popovych, I., Safonov, M., Palamarchuk, I., Blah, V.: Decision support during the vessel control at the time of negative manifestation of human factor. In: Proc. of the 3th International Workshop on Computer Modeling and Intelligent Systems (CMIS-2020), Zaporizhzhia (2020). http://ceur-ws.org/Vol-2608/paper2.pdf
8. Nosov, P. S., Ben, A. P., Mateichuk, V. N., Safonov, M. S.: Identification of "Human error" negative manifestation in maritime transport. Radio Electronics, Computer Science, Control 4(47):204-213 (2018). DOI: 10.15588/1607-3274-2018-4-20
9. Nosov, P., Palamarchuk, I., Zinchenko, S., Popovych, I., Nahrybelnyi, Y., Nosova, H.: Development of means for experimental identification of navigator attention in ergatic systems of maritime transport. Bulletin of University of Karaganda. Technical Physics 1(97):58-69 (2020). DOI: 10.31489/2020Ph1/58-69
10. Germanischer Lloyd SE: Rules for Classification and Construction Ship Technology (2013)
11. Hubert, F.: Dynamic Positioning Systems: Principles, Design and Applications Editions OPHRYS p.189 (1990)
12. Perez, T.: Dynamic Positioning Marine Manoeuvring (2017). DOI: 10.1002/9781118476406.emoe110
13. Pakaste, R., Laukia, K., Wilhelmson, M., Kuuskoski, J.: Experience with Azipod®propulsion systems on board marine vessels. Marine Propulsion. https://pdfs.semanticscholar.org/4956/a88815fe21a86883277042d8cd304a35efc5.pdf
14. Piloting Vessels Fitted with Azimuthing Control Devices (ACD's). United Kingdom Maritime Pilot's Association (UKMPA Transport House London)
15. Podder, T. K., Sarkar, N.: Fault – tolerant control of an autonomous underwater vehicle under truster redundancy. Robotics and Autonomous Systems 34(1):39-52 (2001)
16. Zemlyakov, A. S.: Control the angular position of a spacecraft with an excess gyrodin structure. Bulletin of Kazan State Technical University 4:56-62 (2001)

17. Lebedev, D. V.: Momentum unloading excessive reaction-wheel system of a spacecraft. Journal of Computer and Systems Sciences International 47(4):613-620 (2008)
18. Gao, W., Tang, Q., Yao, J., Yang, Y.: Automatic motion planning for complex welding problems by considering angular redundancy. Robotics and Computer-Integrated Manufacturing 62 (2020). DOI: 10.1016/j.rcim.2019.101862
19. Navi – Trainer 5000. Transas offshore simulator. Instructor manual. Transas MIP Ltd (2012)
20. Zinchenko, S. M., captain Tovstokoryi, O. M.: Determination pivot point position and its use for maneuvering the vessel. In: Proc. of the II International Scientific and Practical Maritime Conference of the Department of Power Plants and TE of Odessa National Maritime University MPP & O-2020, Odessa (2020).
21. Artyszuk, J.: Pivot point in ship manoeuvring. Scientific Journals Maritime University of Szczecin. 20(92):13-24.
22. Seo, S. G.: The Use of Pivot Point in Ship Handling for Safer and More Accurate Ship Manoeuvring. In: Proc. of IMLA 1(29):271-280 (2011).
23. Butusina, P., Dinu, D.: Ship’s Pivot Point in current and swell. http://www.pilotmag.co.uk/wp-content/uploads/2012/01/Pivot-point-final.pdf
24. Seo, S. G.: Safer and More Efficient Ship Handling with the Pivot Point Concept. The International Journal on Marine Navigation and Safety of Sea Transportation 10(4):605-612 (2016). DOI: 12.12716/1001.10.04.09
25. Wedad, A. S., Abdulqader, M. M.: New Caledonian crow learning algorithm: A new metaheuristic algorithm for solving continuous optimization problems. Applied Soft Computing (2020). DOI:10.1016/j.asoc.2020.106325
26. Satnam, K., Lalit, K. A., Sangal, A. L., Gaurav, D.: Tunicate Swarm Algorithm: A new bio-inspired based metaheuristic paradigm for global optimization. Engineering Applications of Artificial Intelligence 90 (2020). DOI: 10.1016/j.engappai.2020.103541
27. Barman, R.: Optimization of Ship steering control system using Genetic Algorithms. Department of Ocean Engineering & Naval architecture Indian Institute of Technology (2020)
28. Zinchenko, S. M, Matejchuk, V. M., Lyashenko, V G., Ben, A. P., Tovstokoryi, O. M., Grosheva, O. O.: The method of using training equipment for the development and testing of ship motion control systems. Patent of Ukraine № 133709 (2019)
29. Zinchenko, S. M, Nosov, P. S, Mateichuk, V. M, Mamenko, P. P, Grosheva, O. O.: Use of navigations simulators for development and testing ship control systems. In: Proc. of the International scientific and practical conference dedicated to the memory of professors Fomin Yu. Ya and Semenov V. S., 350-355, Odessa (2019)
30. Navi – Trainer Professional 5000 (version 5.35). Instructor manual (2014)